

# Small pitch-angle magnetobremsstrahlung in inhomogeneous curved magnetic fields

S.R. Kelner\* and F.A. Aharonian†

The character of radiation of relativistic charged particles in strong magnetic fields largely depends on the disposition of particle trajectories relative to the field lines. The motion of particles with trajectories close to the curved magnetic lines is usually referred to the so-called curvature radiation. The latter is treated within the formalism of synchrotron radiation by replacing the particle Larmor radius with the curvature radius of the field lines. However, even at small pitch angles, the curvatures of the particle trajectory and the field line may differ significantly. Moreover, as we show in this paper the trajectory curvature varies with time, i.e. the process has a stochastic character. Therefore for calculations of observable characteristics of radiation by an ensemble of particles, the radiation intensities should be averaged over time. In this paper, for determination of particle trajectories we use the Hamiltonian formalism, and show that close to curved magnetic lines, for the given configuration of the magnetic field, the initial point and particle energy, always exist a *smooth trajectory* without fast oscillations of the curvature radius. This is the trajectory which is responsible for the curvature radiation. The realization of this regime requires the initial particle velocity to be directed strictly along the smooth trajectory. If initially the velocity vector is adjacent to the field line or close to it, a transition of the particle to the smooth trajectory on a later stage cannot be excluded, however under certain conditions this can happen only after the particle has already radiated out all its energy. Even for an initial narrow angular distribution of the particle beam, the energy spectrum of the resulting radiation appears significantly harder compared to the energy spectrum of the curvature radiation. This result might have direct relation to the recent spectral measurements of gamma-radiation of pulsars by the *Fermi* Gamma-ray Space Telescope.

PACS numbers: 41.60.Ap, 41.60.-m, 95.30.Gv

## I. INTRODUCTION

The motion of a relativistic charged particle in a strong magnetic field is accompanied by a radiation which in general terms can be called magnetobremsstrahlung. While moving in a homogeneous field, the particle energy is gradually radiated away, however, its velocity component  $v_{\parallel}$  parallel to the magnetic field remains unchanged. Indeed, this statement is obvious for  $v_{\parallel} = 0$ , therefore in an arbitrary coordinate system which moves along (or opposite) the magnetic field, we have  $v_{\parallel} = \text{const}$ . Therefore,

$$\frac{c^2}{v_{\parallel}^2} - 1 = \frac{p_{\perp}^2 + m^2 c^2}{p_{\parallel}^2} = \text{const}, \quad (1)$$

where  $p_{\parallel}$  and  $p_{\perp}$  are the parallel and perpendicular components of the momentum, respectively. This equation allows us to find the remaining energy of the particle, after the radiative damping of the perpendicular component of motion. Let us denote the initial and final values of the parallel and perpendicular components of the momentum as  $p_{\parallel}$ ,  $p_{\perp}$ , and  $p'_{\parallel}$ ,  $p'_{\perp} = 0$ , respectively. From

Eq.(1) follows that

$$p'_{\parallel} = p_{\parallel} \frac{mc}{\sqrt{p_{\perp}^2 + m^2 c^2}}. \quad (2)$$

If the initial perpendicular momentum is nonrelativistic,  $p_{\perp} \ll mc$ , then  $p'_{\parallel} \approx p_{\parallel}$ , i.e. the damping of the perpendicular motion does not have an impact on the particle energy. However, for  $mc \ll p_{\perp} \ll p_{\parallel}$ , we have  $p'_{\parallel} \ll p_{\parallel}$ , i.e. during the damping of the perpendicular motion the particle loses almost all its energy. At  $p_{\perp} \gg mc$ , the momenta  $p_{\parallel}$  and  $p_{\perp}$  vary similarly with time since the ratio  $p_{\perp}/p_{\parallel} = \text{const}$  (see Eq.(2)). The constant ratio of  $p_{\perp}/p_{\parallel}$  has the following explanation. The ultrarelativistic particle emits photons within the angle  $\lesssim 1/\gamma$  in the direction of its momentum  $\mathbf{p}$ , therefore in the case of  $1/\gamma \ll p_{\perp}/p_{\parallel}$ , one may assume that the recoil momentum is directed opposite to the vector  $\mathbf{p}$ .

The radiation of charged particles in strong magnetic fields is determined by the character of their motion, in particular by the disposition of particle trajectories relative to the field lines. As we show in this paper, in the close vicinity of curved field lines should exist a special trajectory the particle motion along which is not accompanied by perpendicular oscillation. We call this trajectory as *smooth trajectory*. In the case of homogeneous magnetic field the smooth trajectory is a straight line parallel to the field line. The initial short interval of the smooth trajectory in the curved magnetic field can be treated as a circle with a radius close to the curvature radius of the field line. An ultrarelativistic particle moves steadily along this circle, therefore for calculations of the accompanying radiation one can apply the well known

\* National Research Nuclear University (MEPHI), Kashirskoe shosse 31, 115409 Moscow, Russia; Max-Planck-Institut für Kernphysik, Saupfercheckweg 1, D-6917 Heidelberg, Germany; skelner@rambler.ru

† Dublin Institute for Advanced Studies, 31 Fitzwilliam Place, Dublin 2, Ireland; Max-Planck-Institut für Kernphysik, Saupfercheckweg 1, D-6917 Heidelberg, Germany; Felix.Aharonian@mpi-hd.mpg.de

formulae, and the radiation itself can be considered as a *curvature radiation*.

In the case of large pitch-angles in the curved inhomogeneous magnetic field, the inhomogeneity does not affect the radiation if the Larmor radius is small compared to the curvature of the field lines, and to the characteristic distance scale on which the field is noticeably changed. This case corresponds to the regime of *synchrotron radiation*. All formulae that describe the synchrotron and curvature radiation regimes coincide if we present them in the terms of the trajectory curvature radius  $R_c$ .

For small pitch angles the picture can be essentially different. Let us assume that initially the velocity vector is parallel to the field line. Then, the acceleration  $\mathbf{a}|_{t=0} = 0$ , correspondingly the curvature radius<sup>1</sup>  $R_c|_{t=0} = \infty$ , thus no radiation take place at  $t = 0$ . In the curved magnetic field, a rectilinear uniform motion is not possible, therefore an acceleration and radiation of the particle are unavoidable, and, what is essential for the correct treatment of the problem, the acceleration and the curvature radius appear to be time-dependent. In this paper we show that this is true for all trajectories located close to the *smooth trajectory*. This implies that the radiation also varies with time, thus for calculations of measurable characteristics of radiation one should average the relevant distributions over time.

It is generally believed that for the initially small pitch angles the charged particles rapidly radiate away the fraction of their energy related to the component of the momentum perpendicular to the field line, i.e. the perpendicular motion quickly disappears, and particles move along the field lines (see e.g. Ref. [1]). However, here one should distinguish two different cases. Let  $p_{\parallel}$  and  $p_{\perp}$  be the particle momentum components parallel and perpendicular to the smooth trajectory, respectively. Let us assume that  $p_{\parallel} \gg mc$  and  $p_{\parallel} \gg p_{\perp}$ . If  $p_{\perp} \ll mc$ , then the perpendicular component of motion is quickly damped; the particle will continue to move along the smooth trajectory and thus emit curvature radiation. However, if  $p_{\perp} \gg mc$ , then as in the case of the uniform magnetic field,  $p_{\parallel}$  and  $p_{\perp}$  will be reduced with the same time-dependency. The calculations of characteristics of the resulting radiation, which is different from both synchrotron and curvature radiation components, is the prime objective of this paper. We call this regime of radiation as *small pitch angle magnetobremssstrahlung*.

## II. THE SMOOTH AND CLOSE TO THEM TRAJECTORIES

We start with the analysis of motion of ultrarelativistic particle in a simple model which allows exact solutions. Namely, below we consider the case when the

magnetic field has the same symmetry as the field of an infinitely long straight wire. Then, in the cylindrical system of coordinates,  $(r, \phi, z)$ , the field has only an azimuthal component; it depends only on the distance to the axis of symmetry,  $r$ , but not on  $z$  and  $\phi$ . We denote by  $(\mathbf{e}_r, \mathbf{e}_{\phi}, \mathbf{e}_z)$  a moving system of unit vectors linked to the point  $(r, \phi, z)$ . The magnetic field can be expressed in the form  $\mathbf{B} = B(r) \mathbf{e}_{\phi}$ . The field lines are circles of radius  $r$ . It appears that particles in such a field can move along trajectories close to the circular field lines.

The equation that describes the particle motion in the magnetic field is

$$m\gamma\dot{\mathbf{v}} = \frac{e}{c}(\mathbf{v} \times \mathbf{B}). \quad (3)$$

Let us find a solution for which  $r = r_0 = \text{const}$ , and the velocity

$$\mathbf{v} = v_{\phi}\mathbf{e}_{\phi} + v_z\mathbf{e}_z. \quad (4)$$

Note that the components  $v_{\phi}$  and  $v_z$  are constants. The vector  $\mathbf{e}_{\phi}$  is uniformly rotating with an angular frequency  $\omega = v_{\phi}/r_0$ , therefore the derivative  $d\mathbf{e}_{\phi}/dt = -v_{\phi}\mathbf{e}_r/r$ , and the vector  $\mathbf{e}_z = \text{const}$ . Substituting Eqs. (4) into (3), we find

$$m\gamma\frac{v_{\phi}^2}{r_0}\mathbf{e}_r = \frac{e}{c}v_zB\mathbf{e}_r. \quad (5)$$

From here follows that

$$\frac{v_z}{v_{\phi}} = \frac{mcv_{\phi}\gamma}{eBr_0}. \quad (6)$$

Writing the velocity components in the form  $v_z = v \sin \alpha$ ,  $v_{\phi} = v \cos \alpha$  (the angle starts from the “equator”, i.e.  $-\pi/2 \leq \alpha \leq \pi/2$ ), and expressing the velocity  $v$  via Lorentz factor, Eq.(6) can be presented in the following form

$$\frac{\sin \alpha}{\cos^2 \alpha} = \frac{mc^2\gamma}{eBr_0} \sqrt{1 - 1/\gamma^2}. \quad (7)$$

Apparently, for any given  $\gamma$  this equation defines the angle  $\alpha$ . Eq.(3) indeed has solutions in the form of Eq.(4) which describe the helicoidal motion depending of parameters  $\gamma$  and  $r_0$ . Note that motion of particles with strictly circular trajectories is not possible.

The condition for a small step in the helix,  $|\alpha| \ll 1$ , requires

$$1 \ll \gamma \ll \frac{|e|Br_0}{mc^2} = 6 \times 10^{13} \left( \frac{B}{10^{11} \text{ G}} \right) \left( \frac{r_0}{10 \text{ km}} \right). \quad (8)$$

Note that typical for pulsars values of  $B$  and  $r_0$  readily satisfy this condition. Then,

$$\alpha = \frac{mc^2\gamma}{eBr_0}; \quad |\alpha| \ll 1, \quad (9)$$

thus the particle trajectory can be interpreted as a motion along the field line with a simultaneous drift in

<sup>1</sup> Note that at the motion with a constant absolute speed value, the curvature radius is equal, by definition, to  $R_c = v^2/|\mathbf{a}|$ .

the perpendicular direction. The positive and negative charges drift in opposite directions. Under the condition of Eq.(8), the curvature radius  $R_c$  of a particle located at the distance  $r_0$ , does not depend on the particle energy and practically coincides with the curvature radius of the field line  $r_0$ . Note that this conclusion is correct for any configuration of the magnetic field. Indeed, the short segments of the field line can be treated as a circle, therefore when satisfying the condition of Eq.(8), always exist trajectories which (or at least their initial segments) are very close (but not identical) to the field line. In the Introduction, such trajectories have been called smooth trajectories. Also as indicated above, the magnetobremstrahlung of a particle moving along a smooth trajectory should be considered as the strict definition of the curvature radiation. Its intensity is defined as

$$I_{\text{curv}} = \frac{2e^2c}{3} \frac{\gamma^4}{R_c^2} \approx \frac{2e^2c}{3} \frac{\gamma^4}{r_0^2}. \quad (10)$$

When the particle moves close to but not exactly along the smooth trajectories, the radiation intensity can deviate from Eq.(10). Therefore one should investigate the trajectories in the vicinity of the smooth trajectories.

For this purpose it is convenient to use the Hamiltonian formalism. The vector potential can be taken in the form  $A_x = 0$ ,  $A_y = 0$ ,  $A_z = A(r)$ , therefore the azimuthal component of the field  $B(r) = -dA/dr$ . In the cylindrical coordinates the Hamilton function can be written as

$$H = c \sqrt{P_r^2 + \frac{P_\phi^2}{r^2} + (P_z - \frac{e}{c} A(r))^2 + m^2 c^2}, \quad (11)$$

where  $P_r$ ,  $P_\phi$  and  $P_z$  are the generalized momenta corresponding to the coordinates  $r$ ,  $\phi$  and  $z$ . Because of the azimuthal symmetry of the magnetic field and its homogeneity along the  $z$  axis,  $\phi$  and  $z$  are cyclic coordinates. Therefore  $P_\phi$  and  $P_z$ , as well as the energy, are integrals of motion. The presence of three integrals of motion allows us to reduce the problem to the one-dimensional case, and thus comprehensively study the qualitative behavior of the solutions. Below we will limit the treatment of the problem by the case of ultrarelativistic particles and small pitch-angles.

For given  $P_\phi$  and  $P_z$ , the radial motion can be considered, as it follows from Eq.(11), as a motion in the field with the following effective potential:

$$U_{\text{eff}}(r) = \frac{P_\phi^2}{r^2} + (P_z - \frac{e}{c} A(r))^2. \quad (12)$$

The first and second derivatives of this potential are

$$U'_{\text{eff}}(r) = -\frac{2P_\phi^2}{r^3} + \frac{2e}{c} B(r) (P_z - \frac{e}{c} A(r)), \quad (13)$$

and

$$U''_{\text{eff}}(r) = \frac{6P_\phi^2}{r^4} + \frac{2e}{c} B'(r) (P_z - \frac{e}{c} A(r)) + \frac{2e^2}{c^2} B^2(r). \quad (14)$$

Assuming that at  $r = r_0$  the derivative  $U'_{\text{eff}}(r_0) = 0$ , then at this point

$$P_z - \frac{e}{c} A(r_0) = \frac{cP_\phi^2}{r_0^3 e B(r_0)}, \quad (15)$$

$$U''_{\text{eff}}(r_0) = \frac{2P_\phi^2}{r_0^4} \left( 3 + \frac{r_0 B'(r_0)}{B(r_0)} \right) + \frac{2e^2}{c^2} B^2(r_0). \quad (16)$$

If  $B$  decreases with  $r$  as a power-law,  $B \sim 1/r^\delta$ , then for  $\delta < 3$  the both terms in Eq.(16) are positive, therefore  $U_{\text{eff}}$  has a minimum at  $r_0$ . Furthermore, assuming that the condition of Eq.(8) is fulfilled, in Eq.(16) we can keep only the last term.

For integration of the equations of motions we apply the standard method which is used in the theory of small oscillations. In the vicinity of the minimum point the function  $U_{\text{eff}}(r)$  is approximated by a parabola:

$$U_{\text{eff}}(r) = P_0^2 + m^2 \omega_c^2 (r - r_0)^2, \quad (17)$$

where

$$\omega_c^2 = \frac{1}{2m^2} U''_{\text{eff}}(r_0) \approx \left( \frac{eB(r_0)}{mc} \right)^2, \quad (18)$$

$$P_0^2 = U_{\text{eff}}(r_0) = \frac{P_\phi^2}{r_0^2} \left( 1 + \frac{P_\phi^2}{r_0^4 m^2 \omega_c^2} \right). \quad (19)$$

In these denotations, the Hamilton function can be presented in the form

$$H = c \sqrt{P_r^2 + m^2 \omega_c^2 (r - r_0)^2 + P_0^2 + m^2 c^2}, \quad (20)$$

and correspondingly the equations of motion are

$$\dot{r} = \frac{\partial \tilde{H}}{\partial P_r} = \frac{c^2 P_r}{E}, \quad \dot{P}_r = -\frac{\partial \tilde{H}}{\partial r} = -\frac{m^2 c^2 \omega_c^2}{E} (r - r_0), \quad (21)$$

where  $E$  is the particle energy. The solution of these equations gives

$$r = r_0 - \rho \cos \frac{\omega_c t}{\gamma}, \quad P_r = m \rho \omega_c \sin \frac{\omega_c t}{\gamma}, \quad (22)$$

where  $\gamma = E/(mc^2)$  is the Lorentz factor of the particle,  $\rho$  is an arbitrary constant<sup>2</sup> related to the particle energy through the relation

$$E = c \sqrt{P_0^2 + m^2 \rho^2 \omega_c^2 + m^2 c^2}. \quad (23)$$

<sup>2</sup> Note that here the origin of the coordinate system is arbitrary, therefore instead of  $t$  one can use  $t - t_0$ , where  $t_0$  is the second arbitrary constant. Below we omit the arbitrary constants which can be added to  $\phi$  and  $z$ .

The condition of applicability of Eq.(22) is the smallness of  $\rho$  compared to  $r_0$  as well as to the characteristic linear scale on which the magnetic field is changed significantly.

Now we should find the time-dependencies of other coordinates. In this regard we note that

$$\dot{\phi} = \frac{\partial H}{\partial P_\phi} = \frac{P_\phi}{m\gamma} \frac{1}{r^2} \approx \frac{P_\phi}{m\gamma} \frac{1}{r_0^2} \left( 1 - \frac{2(r-r_0)}{r_0} \right). \quad (24)$$

Using Eq.(22), we find

$$\dot{\phi} = \frac{P_\phi}{m\gamma} \frac{1}{r_0^2} \left( 1 + \frac{2\rho}{r_0} \cos \frac{\omega_c t}{\gamma} \right), \quad (25)$$

$$\phi = \frac{P_\phi}{m\gamma} \frac{1}{r_0^2} \left( t + \frac{2\rho\gamma}{\omega_c r_0} \sin \frac{\omega_c t}{\gamma} \right). \quad (26)$$

Now substituting in

$$\dot{z} = \frac{\partial H}{\partial P_z} = \frac{c^2}{E} \left( P_z - \frac{e}{c} A(r) \right) \quad (27)$$

the following approximate presentation for  $A(r)$ ,

$$A(r) = A(r_0 + (r-r_0)) \approx A(r_0) - B(r_0) \cdot (r-r_0), \quad (28)$$

and using Eqs. (15) and (22), we find

$$\dot{z} = \frac{P_\phi^2}{\gamma \omega_c m^2 r_0^3} - \frac{\rho \omega_c}{\gamma} \cos \frac{\omega_c t}{\gamma}, \quad (29)$$

$$z = \frac{P_\phi^2}{\gamma \omega_c m^2 r_0^3} t - \rho \sin \frac{\omega_c t}{\gamma}. \quad (30)$$

In order to make the analytical expressions more convenient to work with, it is useful to use instead of  $P_\phi$  and  $\rho$  the following parameters  $\beta_\parallel$  and  $\beta_\perp$  which are determined as

$$\beta_\parallel = \frac{P_\phi}{mc\gamma r_0}, \quad \beta_\perp = \frac{\rho \omega_c}{\gamma c}, \quad (31)$$

and denote

$$\beta_D = \frac{P_\phi^2}{c\gamma \omega_c m^2 r_0^3} = \frac{c\gamma \beta_\parallel^2}{r_0 \omega_c}. \quad (32)$$

Since  $P_\phi$  is the projection of the particle momentum on the axis  $z$ , then  $\beta_\parallel$  is the component of the velocity parallel to the magnetic field (in units of  $c$ ), and  $\beta_\perp$  is the perpendicular components of the velocity. Finally  $\beta_D$  is the drift velocity.

For the new variables we find

$$\dot{r}/c = \beta_\perp \sin \tau, \quad \dot{z}/c = \beta_D - \beta_\perp \cos \tau, \quad (33)$$

$$\dot{\phi} = \frac{\beta_\parallel c}{r_0} \left( 1 + \frac{2\beta_\perp \beta_D}{\beta_\parallel^2} \cos \tau \right), \quad (34)$$

where  $\tau = \omega_c t/\gamma$ ; azimuthal component of velocity is

$$v_\phi = r\dot{\phi} = c\beta_\parallel \left( 1 + \frac{\beta_\perp \beta_D}{\beta_\parallel^2} \cos \tau \right). \quad (35)$$

For  $\beta_\perp = 0$ , this solution coincides with the obtained above exact solution that describes the motion along a smooth trajectory (in this case, along the helicoidal line). The same trajectory can be found if we average Eqs.(33)-(35) over time. Therefore this solution can be interpreted as a motion along the spiral around the smooth trajectory. At  $\beta_\perp \neq 0$ , the solution is approximate; it is correct when the following condition is fulfilled:

$$\beta_\perp \ll \beta_\parallel, \quad \beta_D \ll \beta_\parallel. \quad (36)$$

The relation between  $\beta_\perp$  and  $\beta_D$  can be arbitrary. Since  $\beta_\parallel \approx 1$ , the second of the above conditions is equivalent to Eq.(8). The same requirement can be formulated in terms smallness of the Larmor radius compared to the curvature radius of the field line.

Note that the inclusion of the process of the *gradient drift* into consideration hardly can be justified since it would exceed the accuracy of the approach. Indeed, the gradient drift would appear in the formulae if one adds in Eq.(28) the next (quadratic) term of expansion, while our study is limited for the linear terms. Therefore throughout the paper we will take into account only the curvature drift.

For the chosen new variables, the velocity and its square are

$$\mathbf{v} = \dot{r}\mathbf{e}_r + r\dot{\phi}\mathbf{e}_\phi + \dot{z}\mathbf{e}_z, \quad (37)$$

and

$$v^2 = c^2 \left( \beta_\parallel^2 + \beta_\perp^2 + \beta_D^2 \right). \quad (38)$$

Note that  $v^2$  does not depend on  $t$ . In order to find the acceleration, we use the following equation

$$\mathbf{a} = \frac{e}{mc\gamma} (\mathbf{v} \times \mathbf{B}) = \frac{\omega_c}{\gamma} (\dot{r}\mathbf{e}_z - \dot{z}\mathbf{e}_r), \quad (39)$$

where it is taken into account that the field has only an azimuthal component. The square of the acceleration

$$a^2 = a_0^2 \left( 1 - \frac{2\beta_\perp}{\beta_D} \cos \tau + \frac{\beta_\perp^2}{\beta_D^2} \right), \quad (40)$$

where  $a_0 = c^2 \beta_\parallel^2 / r_0$ . This equation can be derived also through the consideration of kinematics. Indeed,

$$\mathbf{a} = \ddot{\mathbf{r}} = (\ddot{r} - r\dot{\phi}^2)\mathbf{e}_r + (2\dot{r}\dot{\phi} + r\ddot{\phi})\mathbf{e}_\phi + \ddot{z}\mathbf{e}_z. \quad (41)$$

From here, due to the smallness of the ratios  $\beta_\perp/\beta_\parallel$  and  $\beta_D/\beta_\parallel$ , we obtain an equation identical to Eq.(40).

At  $\beta_\perp = 0$  we have  $a^2 = a_0^2 = \text{const}$ . This is the case when the particle moves along the smooth trajectory. For  $\beta_\perp = \beta_D$ , the acceleration  $a^2 = 2a_0^2(1 - \cos \tau)$ . For the moments of time, when the acceleration becomes zero, the particle velocity is parallel to the field line. In the limit of  $\beta_\perp \gg \beta_D$ , the acceleration does not depend on the radius of the field curvature and on time:

$$a^2 = a_0^2 \frac{\beta_\perp^2}{\beta_D^2} = \left( \frac{c\beta_\perp \omega_c}{\gamma} \right)^2. \quad (42)$$

It is well known (see e.g. Ref. [2]) that this equation describes also the acceleration of the particle in the homogeneous magnetic field. For applicability of Eq.(42) it is sufficient to fulfill only the condition  $\beta_{\perp} \gg \beta_D$ , while the relation between  $\beta_{\perp}$  and  $\beta_{\parallel}$  can be arbitrary.

For an ultrarelativistic particle, the curvature radius of trajectory and the acceleration are linked with a simple relation  $|\mathbf{a}| = c^2/R_c$ , which at  $v = c$  is, in fact, the definition of the curvature radius. Thus, the radius of the curvature of trajectory is

$$R_c(t) = r_0 \left( 1 - \frac{2\beta_{\perp}}{\beta_D} \cos \tau + \frac{\beta_{\perp}^2}{\beta_D^2} \right)^{-1/2}. \quad (43)$$

Here  $\beta_{\parallel}$  is set to be equal to 1 given that  $1 - \beta_{\parallel} \ll 1$ .

Let us consider now the motion of the charged particle in the field of a magnetic dipole (the so-called Störmer problem). Such a system appears to be (unlike the previous case) non-integrable (see e.g. Ref. [3]), and generally it is impossible to conduct even a qualitative analysis of the motion. However, when the condition of Eq.(8) is fulfilled, the system has smooth trajectories. The trajectories in the close vicinity of the latter present lines spiraling around the smooth trajectories, i.e. basically we deal with the same picture as discussed above for the straight wire. This is confirmed also by our numerical calculations.

In Fig. 1 we show the initial part of the trajectory in the field of magnetic dipole directed towards the  $z$ -axis. At the initial moment of time the particle is located in the point  $\mathbf{r}(0) = (\sin \vartheta, 0, \cos \vartheta)$  where the coordinates are measured in units of the radius of the object (star),  $R_*$ , the angle  $\vartheta = 20^\circ$ , the initial velocity is directed along the field line, and the parameter  $\xi = 10^{-3}$  (see Appendix A). The amplitude of oscillations appears of the same order of magnitude, i.e.  $10^{-3}$ , therefore in the left panel of Fig. 1 the oscillations are not visible. Fig. 2 shows the dependence of acceleration on time. The period of oscillations is equal to  $T_0 = 2\pi mc\gamma/(eB_0)$ , where  $B_0$  is the magnetic field on the surface of the star. The decrease of the amplitude and the increase of the period is due to the reduction of the field along the trajectory. The change of the Lorentz factor  $\gamma$  due to the radiation losses is not taken into account. The trajectory patters for larger time intervals are discussed in Appendix.

It should be noted that the necessity of calculations of characteristics of (synchro-bremsstrahlung) radiation in the context of proper treatment of trajectories of charged particles in curved magnetic fields, has been correctly indicated also in Ref. [4]. However, our analysis shows that some of the basic results and conclusions of that paper appear to be not correct. Therefore for clarification of some issues of conceptual character, below we compare the results of the present study with the relevant result from Ref. [4]. For convenience, the equations from Ref. [4] will be referred by their original numbers with an additional indication of [4].

Let us compare, in particular, the results of calculations regarding the square of the acceleration,  $\mathbf{a}^2$ , in the

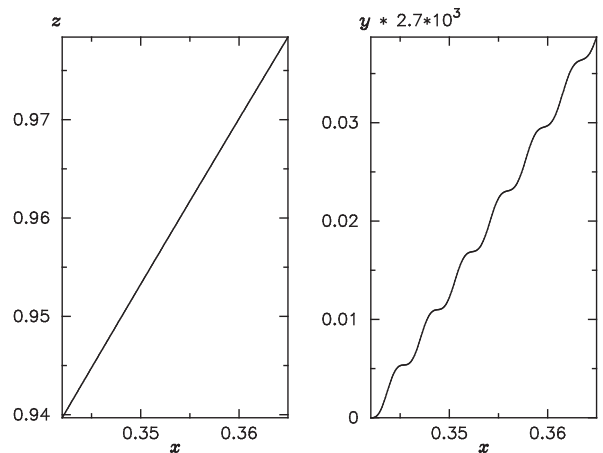


FIG. 1. The initial segment of the trajectory of charged particle in the field of the magnetic dipole. The initial point is located on the surface of the star at the angle  $20^\circ$  relative to the  $z$ -axis, the initial velocity is directed along the field line. The  $y$ -axis in the right panes is rescaled (multiplied by a factor of  $2.7 \times 10^3$  in order to make visible the oscillations.

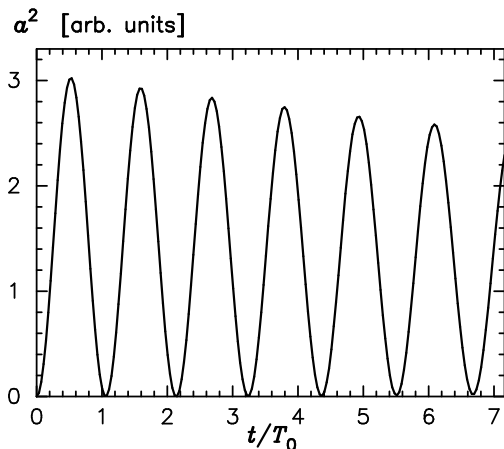


FIG. 2. The time-dependence of acceleration during the motion of a charged particle along the trajectory presented in Fig.1

curved magnetic field. For the denotations used in this paper, the equation (5,[4]) can be written in the form

$$\mathbf{a}^2 = a_0^2 \left( 1 + \frac{\beta_{\perp}}{\beta_D} \right)^2. \quad (44)$$

This equation is not correct; in particular it lacks time-dependence. Apparently, the error in Ref. [4] has appeared because of the definition of acceleration for which the authors used a wrong formula given by equation (1,[4]). The reference to the monograph of Jackson [5], as an original source of this equation is misleading. The monograph [5] does contain derivation of the drift velocity. The second term in (1,[4]) in fact is the drift velocity  $\mathbf{v}_D$  (Eq.(12.117) from Ref. [5]). In the derivation of  $\mathbf{v}_D$

a time-averaging procedure was applied, thus all oscillating terms have been canceled. If we are interested only in the systematic shift (drift), these terms, of course, do not affect the result. However if one wants to calculate the radiation of particles, then the oscillating terms cannot be ignored. Correspondingly, the velocity  $\mathbf{v}(t)$  cannot be obtained by adding to  $\mathbf{v}_D$  a constant vector (of unknown direction!)  $\mathbf{v}_0$ , as it is done in Ref. [4].

It should be noted that in some cases the replacement of  $\mathbf{v}(t)$  by a constant vector should not necessarily lead to a wrong results. For example, from the solution of the equation for the motion in the constant homogeneous field follows that  $\mathbf{a}^2 = \text{const}$ , therefore for definition of  $\mathbf{a}^2$ , we can ignore the velocity's time-dependence. We would like to emphasize that one can make such a statement only when the solution of the equation motion is known. In more complex cases, like the one analyzed above, the solution of the equation of motion is a necessary step. Any *a priori* assumption that  $\mathbf{a}^2(t) = \text{const}$  may lead to incorrect results. In this regard, all equations in Ref.[4], which contain  $\mathbf{a}^2$  are not correct. The results of this work can be considered, in the best case, as interpolations of two well known cases:  $\beta_\perp \ll \beta_D$  (curvature radiation) and  $\beta_\perp \gg \beta_D$  (synchrotron radiation). In these limiting cases the results of Eqs. (44) and (40) coincide. The reason of this agreement is explained above.

Finally, we note that Ref. [4] contains another incorrectness related to the derivation of Eq.(21,[4]). Although the authors do cite to the classical paper of J. Schwinger [6], apparently they have missed to mention that not only the final result (i.e. the equation (21,[4]) itself), but also all intermediate steps for derivation of this equation (using the same method and the same denotations) have been already obtained in Schwinger's paper.

### III. INTENSITY AND ENERGY SPECTRUM OF RADIATION

In this section we calculate, within the framework of classical electrodynamics, the intensity and the energy spectrum of radiation of a charged ultrarelativistic particle with the perpendicular component of velocity  $\beta_\perp \sim \beta_D$ . If the radius of the curvature of the trajectory  $R_c \sim r_0$ , the characteristic energy of the emitted photon is  $\sim \hbar c \gamma^3 / r_0$ . The requirement of smallness of this energy compared to the energy of the particle  $mc^2 \gamma$  (the condition of applicability of classical electrodynamics) implies  $\hbar \gamma^2 \ll m c r_0$ . We assume that the perpendicular (relative to the smooth trajectory) momentum  $p_\perp \ll p_\parallel$ , but, at the same time,  $p_\perp \gg mc$ . Using Eq.(32), the latter inequality can be presented in the form  $c \gamma^2 \gg \omega_c r_0$ . This gives the following constraint on the Lorentz-factor:

$$\omega_c r_0 / c \ll \gamma^2 \ll m c r_0 / \hbar. \quad (45)$$

The condition of smallness of the lower limit compared to the upper limit, implies  $\hbar \omega_c \ll mc^2$ , i.e. the magnetic field should not exceed the critical one,  $B_{\text{cr}} = m^2 c^3 / (e \hbar) = 4.4 \times 10^{13} \text{ G}$ .

The energy radiated away by the particle for a unite interval of time, is [2]

$$I = -\frac{dE}{dt} = \frac{2e^2 \gamma^6}{3c^3} (\mathbf{a}^2 - (\mathbf{v} \times \mathbf{a})^2 / c^2) = \frac{2e^2 c}{3} \frac{\gamma^4}{R_c^2}. \quad (46)$$

Substituting  $R_c$  from Eq.(43), we obtain

$$I = \frac{2e^2 c}{3} \frac{\gamma^4}{r_0^2} (1 - 2\eta \cos \tau + \eta^2), \quad (47)$$

where we introduce a new parameter  $\eta = \beta_\perp / \beta_D$ . The averaged over the period intensity is

$$\langle I \rangle = \frac{2e^2 c}{3} \frac{\gamma^4}{r_0^2} (1 + \eta^2). \quad (48)$$

This formula can be written in the form  $\langle I \rangle = I_{\text{curv}}(1 + \eta^2)$ , where  $I_{\text{curv}}$  is defined in Eq.(10). It is seen that during the motion in the curved magnetic field the curvature radiation has the minimum possible intensity.

In the considered scenario, we deal with three characteristic times. These are the time of energy losses (cooling time),  $t_{\text{cool}} \sim m c r_0^2 / (e^2 \gamma^3)$ , the period of "oscillations",  $T \sim \gamma / \omega_c$ , and the characteristic time of formation of radiation,  $\Delta t \sim r_0 / (c \gamma)$ . It is easy to show, using Eq.(45), that  $\Delta t \ll t_{\text{cool}}$ . Note that this condition is always satisfied in the framework of classical electrodynamics. The ratio  $\Delta t / T \sim \omega_c r_0 / (c \gamma^2)$  also is small compared to 1, as it follows from Eq.(45). Finally, the ratio  $T / t_{\text{cool}} \sim e^2 \gamma^4 / (m c \omega_c r_0^2)$ ; using the lower and upper limits of the Lorentz-factor from Eq.(45), we obtain

$$\alpha \frac{\hbar \omega_c}{mc^2} \ll \frac{T}{t_{\text{cool}}} \ll \alpha \frac{mc^2}{\hbar \omega_c}, \quad (49)$$

where  $\alpha = e^2 / \hbar c \approx 1/137$ .

The smallness of  $\Delta t$  simplifies significantly the calculations of the radiation spectrum. This allows us to ignore the changes of the particle energy and the curvature radius with time, and perform calculations at the fixed "prompt" values of these parameters:  $E(t) = mc^2 \gamma(t)$  and  $R_c(t)$ . Then the spectral flux density of the magnetobremstrahlung integrated over the all emission angles, is described by the well known expression for the synchrotron regime of radiation (see, e.g. Refs. [6], [7])

$$P(\omega, t) = \frac{\sqrt{3} e^2}{2 \pi} \frac{\gamma}{R_c} F\left(\frac{\omega}{\Omega_*}\right). \quad (50)$$

Here

$$\Omega_* = \frac{3c\gamma^3}{2R_c}, \quad (51)$$

and

$$F(x) = x \int_x^\infty K_{5/3}(x') dx', \quad (52)$$

where  $K_{5/3}$  is modified Bessel function. The particle energy loss rate,  $dE/dt = -\int_0^\infty P(\omega, t) d\omega$ ; the calculation of this integral results, as expected, in Eq.(46)

Since  $R_c$  and  $\gamma$  vary with time, the radiation spectrum should be time-dependent as well. Let assume that the condition  $T \ll t_{\text{cool}}$  is satisfied (note that this condition does not contradict to Eq.(49)). Then, since change of  $\gamma$  during the period is small, we can introduce new parameters averaged over time. This in fact has been already done at the changeover from Eq.(47) to Eq.(48), assuming that during the period  $\gamma = \text{const}$ .

By writing  $R_c$ , in accordance with Eq.(43), as

$$R_c = r_0/q(\eta, \tau), \quad q(\eta, \tau) = \sqrt{1 - 2\eta \cos \tau + \eta^2}, \quad (53)$$

the averaged spectral flux density can be presented in the form

$$\langle P(\omega, t) \rangle = \frac{\sqrt{3}e^2}{2\pi} \frac{\gamma}{r_0} G\left(\frac{\omega}{\omega_*}\right). \quad (54)$$

Here

$$G\left(\frac{\omega}{\omega_*}\right) = \frac{1}{\pi} \int_0^\pi q(\eta, \tau) F\left(\frac{\omega}{\omega_* q(\eta, \tau)}\right) d\tau, \quad (55)$$

where  $\omega_* = 3c\gamma^3/(2r_0)$ .  $G$  is a function of two variables:  $x = \omega/\omega_*$  and  $\eta = \beta_\perp/\beta_D$ . If in Eq.(55) we represent the function  $F(x)$  in the form of Eq.(52), and change the order of integration, the integral over  $d\tau$  can be calculated analytically. This allows us to express the function  $G(x)$  in the form of a single integral:

$$G(x) = x \int_{x/(1+\eta)}^\infty K_{5/3}(x') \Psi(x/x') dx', \quad (56)$$

where

$$\Psi\left(\frac{x}{x'}\right) = \begin{cases} \frac{1}{\pi} \arccos \frac{(x/x')^2 - 1 - \eta^2}{2\eta}, & \frac{x}{x'} \geq |1 - \eta|, \\ 1, & \frac{x}{x'} < |1 - \eta|. \end{cases} \quad (57)$$

The function  $G$  for different values of  $\eta$  is shown in Fig. 3. At  $\eta = 0$  (the dot-dashed line) we have a nominal curvature radiation. The curves are based on numerical integration of Eq.(55), using for the function  $F(x)$  the following analytical approximation from Ref. [8],

$$F(x) \approx 2.15 x^{1/3} (1 + 3.06 x)^{1/6} \times \frac{1 + 0.884 x^{2/3} + 0.471 x^{4/3}}{1 + 1.64 x^{2/3} + 0.974 x^{4/3}} e^{-x}, \quad (58)$$

which provides an accuracy better than 0.2% over the entire range of the variable  $x$ . In two limits,  $x \gg 1$  and  $x \ll 1$ , the function  $F(x)$  can be expressed as

$$F(x) \approx 2^{2/3} \Gamma\left(\frac{2}{3}\right) x^{1/3}, \quad x \ll 1, \quad (59)$$

$$F(x) \approx \sqrt{\frac{\pi x}{2}} e^{-x}, \quad x \gg 1. \quad (60)$$

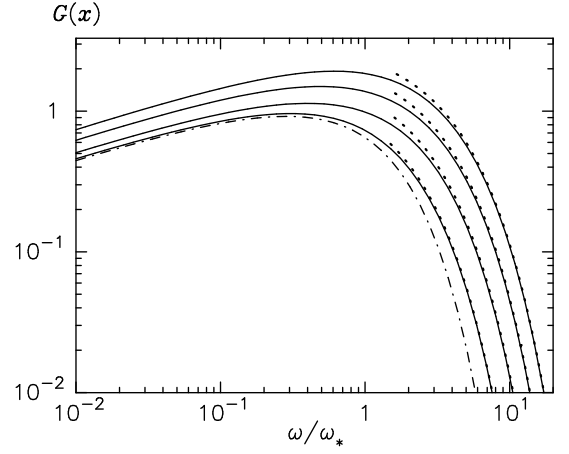


FIG. 3. The spectral flux density of the small pitch-angle radiation averaged over time. The thin solid lines (from top to bottom) correspond to numerical calculations performed for the values of the ratio  $\eta = \beta_\perp/\beta_D = 0, 0.5, 1, 1.5$  and  $2$ . The dotted lines are calculated using the asymptotic presentation of the function  $G(X)$  given by Eq.(62). The dot-dashed line corresponds to the curvature radiation ( $\eta = 0$ ) when the particle moves along the soft trajectory.

Therefore at  $x \ll 1$ , the function  $G(x)$  differs from  $F(x)$  only by a factor which does not depend on  $x$ :

$$G(x) = \frac{1}{\pi} \int_0^\pi (1 - 2\eta \cos \tau + \eta^2)^{1/3} d\tau \times F(x). \quad (61)$$

In the opposite limit,  $x \gg 1$ , the integral can be calculated by using the standard saddle point method. This gives the following asymptotics:

$$G \approx \frac{(1 + \eta)^2}{2\sqrt{\eta}} \exp\left(-\frac{x}{1 + \eta}\right). \quad (62)$$

Formally, in this case the saddle point method can be applied if  $x \gg (1 + \eta)^3/\eta$ . However, the numerical calculations show that in the interval  $0.2 \leq \eta \leq 3$  the simple analytical function given by Eq.(62) provides a good accuracy (better than 10 %) already at  $x \approx 2$  (see Fig. 3).

Let's consider now the case when the injected accelerated electrons are not strictly unidirectional but are distributed within a narrow cone with an opening angle  $\Delta\theta \ll 1$ . We assume that all electrons have the same energy. For the standard synchrotron radiation, a slight change of the pitch angle does not affect the spectrum of radiation. However, in the case of the small pitch-angle magnetobremstrahlung, even a tiny spread of pitch-angles may result in a significant change of the spectrum. It is convenient to express the angular distribution of particles through the parameter  $\eta$ , which is linked to the pitch angle with a simple relation:  $\theta = \eta\beta_D/\beta_\parallel$ . Note that at  $\eta \lesssim 1$ , the pitch angle  $\theta \ll 1$ . For calculations we should specify the angular distribution of particles. Below we consider a Gaussain type distribution:

$$g(\eta) d\eta \sim e^{-\eta^2/(2\zeta)} d\eta, \quad (63)$$

thus the mean value of the square of the perpendicular velocity

$$\langle \beta_{\perp}^2 \rangle = \zeta \beta_D^2. \quad (64)$$

For determination of the energy spectrum we have to average Eq.(55) over time  $\tau$  and parameter  $\eta$ , i.e. calculate the following integral

$$\langle G(x) \rangle = \int_0^\infty d\eta g(\eta) \int_0^\pi \frac{d\tau}{\pi} q(\eta, \tau) F\left(\frac{x}{q(\eta, \tau)}\right). \quad (65)$$

The energy spectra calculated for several values of  $\zeta$  are shown in Fig. 4. Apparently, the case of  $\zeta = 0$  corresponds to the curvature radiation.

As above, using the saddle point method, we can find the asymptotics for  $\langle G \rangle$  at large  $x$ . Rather cumbersome calculations, which we omit here, leads to the following result

$$\langle G(x) \rangle \approx \sqrt{\frac{\zeta}{3x^{1/3}}} \left( x^{1/3} + \zeta^{-1/3} \right)^2 e^{-u}, \quad (66)$$

where

$$u = \frac{3}{2} \zeta^{-1/3} x^{2/3} - \zeta^{-2/3} x^{1/3} + \frac{1}{3\zeta}. \quad (67)$$

This equation is derived under the following conditions:  $x \gg \zeta$  and  $x \gg 1/\zeta$ . However, the comparison of Eq.(67) with accurate numerical calculations show (see Fig. 4), that for  $\zeta \sim 1$  this analytical presentation gives correct results already at  $x \gtrsim 0.5$ .

Although the assumed Gaussian type angular distribution of electrons seems to be a quite reasonable and natural choice in the considered scenario, it would be interesting to investigate the dependence of the radiation spectrum on the specific angular distribution of the electron beam. In particular in Fig.5 we show the radiation spectra calculated for the uniform distribution of electrons within fixed opening angles of the beam. The results shown in Fig.5 (solid curves) are obtained for the same values of the mean square of the perpendicular velocity as in Fig. 4. In Fig.5 we show also the asymptotic solutions given by Eq.(66) for the spectra calculated for the Gaussian type angular distribution (the same dotted curves shown in Fig. 4). The comparison of the results shown in Figs.4 and 5 indicates that the value of the mean square of the perpendicular velocity generally characterizes the energy spectrum of radiation independent of the details of the specific small pitch-angle distribution of electrons.

Note that the spectra of the small-pitch angle radiation do not contain the characteristic exponential term  $e^{-x}$ , as in the case of the synchrotron or curvature radiation, but show a harder behavior. This can be seen from the asymptotics Eq.(67). To demonstrate the tendency of steepening of the energy spectrum beyond the maximum at  $x \sim 1$ , in the table below we show the evolution of

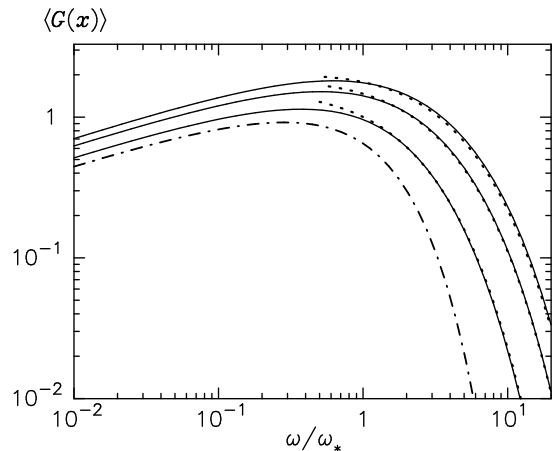


FIG. 4. The spectral flux density of the small-pitch angle radiation averaged over the period and the pitch-angles of particles, assuming a Gaussian type of distribution given by Eq.(63). The solid lines correspond to different values of  $\zeta = \langle \beta_{\perp}^2 \rangle / \beta_D^2$ : 1, 3 and 5 (from bottom to top). The dotted lines are calculated using the asymptotic analytical presentation given by Eq.(66). The dash-dotted line corresponds to the curvature radiation ( $\zeta = 0$ ).

the local slope of the spectral flux density ( the so-called spectral index  $\alpha$ ) which is determined as

$$\alpha = -d(\log \langle G \rangle) / d(\log \omega). \quad (68)$$

It is seen that while in the case of curvature radiation ( $\zeta = 0$ ), the spectrum becomes very steep already at  $x \gtrsim 3$ , in the small-pitch angle radiation regime with  $\zeta = 2$  or  $\zeta = 3$ , a relatively hard spectrum can extend up to  $x \sim 10$ .

$\zeta \backslash x$	2.0	3.0	5.0	10.	20.	30.
0	1.65	2.62	4.59	9.56	19.5	29.5
0.5	1.17	1.67	2.56	4.45	7.56	10.2
1.0	0.96	1.37	2.10	3.63	6.14	8.28
2.0	0.75	1.08	1.67	2.91	4.93	6.65
3.0	0.64	0.93	1.45	2.54	4.31	5.82

#### IV. DISCUSSION

In the context of the motion of an ultrarelativistic charged particle in the strong magnetic field with curved field lines, in the vicinity of the latter always exist trajectories without fast oscillations of the curvature radius. We call them *smooth trajectories*. The angle between the smooth trajectory and the field line appears equal to  $\beta_D$  and is determined by Eq.(32). For the conditions discussed in this paper,  $\beta_D \ll 1$ . This trajectory is distinct in the sense that, strictly speaking, the curvature radiation takes place when the charged particle moves along this trajectory, but not along the magnetic field line as



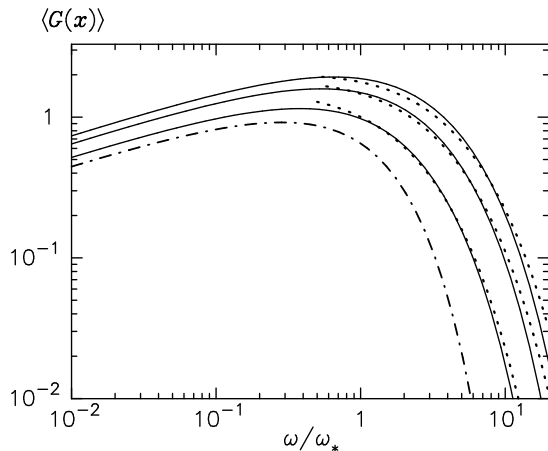


FIG. 5. The spectral flux density of the small-pitch angle radiation averaged over the period and the pitch-angles of particles, assuming a uniform angular distribution of electrons within the opening angle of the beam. The solid lines correspond to different values of the mean square of the perpendicular velocity  $\zeta = \langle \beta_\perp^2 \rangle / \beta_D^2$ : 1, 3 and 5 (from bottom to top). The dotted lines are the same as in Fig4. They are calculated for the Gaussian type of angular distribution using the asymptotic analytical presentation given by Eq.(66). The dash-dotted line corresponds to the curvature radiation ( $\zeta = 0$ ).

it is broadly accepted and discussed in the literature. In fact, if the velocity vector is initially parallel to the magnetic field line, no radiation is possible *by definition*! The curvature radiation appears when the velocity vector becomes parallel to the smooth trajectory. On the other hand, since the curvature radius of the smooth trajectory  $R_c$  is very close to the radius of the field curvature  $r_0$ , the intensity and spectral distribution of the curvature radiation are nevertheless correctly described by the formalism applied in the original papers (see e.g. [1]) where the curvature radiation has been linked to the motion of particles along the magnetic field lines.

Another common misconception in the literature is connected with the belief that the radiation in the strong magnetic field results in prompt damping of the perpendicular component of motion. However, if the perpendicular momentum is ultrarelativistic, the parallel and perpendicular components of the momentum decrease (due to the radiation) by the same law. A strict proof of this statement is possible in the case of homogeneous magnetic field. However, in the context of consideration of direction of the recoil momentum, this feature can be extended to the curved magnetic field for the particle motion along the trajectories close to the smooth trajectory. The fast damping of the perpendicular motion occurs only if the perpendicular component of momentum is non-relativistic. This circumstance might have important practical implications for radiation of highly magnetized relativistic objects.

If initially the velocity vector of the particle is not di-

rected strictly along the smooth trajectory, but at a small angle ( $\theta \ll 1$ ), then for  $\theta\gamma \gg 1$  the perpendicular momentum is ultrarelativistic and the particle moves along the line spiraling around the smooth trajectory (but not the field line). In particular, this happens when initially the velocity is parallel to the field line, provided that  $\gamma\beta_D \gg 1$ . Then, at the initial moment of time  $\mathbf{a} = 0$  and  $R_c = \infty$ . The important difference from the motion in the homogeneous magnetic field is the time-dependence of the curvature radius and the square of acceleration. The radiation in this regime is principally different from both the synchrotron and the curvature radiation regimes. This new regime of the magnetobremstrahlung, which surprisingly has been missed in the previous studies, would be appropriate to call *small pitch-angle radiation*.

The averaged over the period intensity of radiation is given by Eq.(48). It can be presented in the standard form of Eq.(46), if we introduce an *effective* curvature radius  $R_{\text{eff}} = r_0 / \sqrt{1 + \eta^2}$ . However, if we want to have a standard exponential term  $e^{-x}$  in an explicit form (as in the case of the synchrotron or curvature radiation) in the asymptotic presentation for the spectrum given by Eq.(62), the effective curvature radius should be defined differently, namely  $R_{\text{eff}} = r_0 / (1 + \eta)$ . This is another indication of the difference between the small-pitch angle radiation from the synchrotron and curvature regimes of radiation.

The characteristic feature of the small-pitch angle radiation is its strong dependence on the particle angular distribution. Even in the case of a very narrow angular distribution, the radiation spectrum could differ significantly from the unidirectional beam. This is demonstrated in Fig.4 and 5 where the radiation spectra averaged over the pitch-angles of particles, assuming Gaussian type and uniform angular distributions of particles are presented. For the Gaussian type angular distribution, the spectral flux density can be presented in a simple analytical form by Eq.(66) which provides a good accuracy already at  $x \gtrsim 0.5$ . It is seen that the small pitch-angle radiation predicts significantly harder energy spectra compared to the curvature radiation ( $\zeta = 0$ ).

This interesting feature might be a key for interpretation of the recent observations of pulsars by *Fermi* LAT which indicate that the energy spectra of some pulsars, in particular the Crab pulsar [9], in the cutoff region are significantly harder than  $e^{-x}$  as predicted by the curvature radiation models. The energy spectrum of the pulsed emission of the Crab reported in Ref. [9] can be readily described by Eq.(66) assuming  $\zeta = 1$  and a quite reasonable value of the ratio  $\gamma^3/r_0 \simeq 10^{13} \text{ cm}^{-1}$ .

We should note, however, that the formalism developed in this paper cannot be directly used for interpretation of experimental data. It can be applied only at the initial stages, when the energy losses of particles are negligible. Otherwise, for a correct treatment of the time-evolution of particles and their time-dependent radiation, one should solve kinetic equations that describe

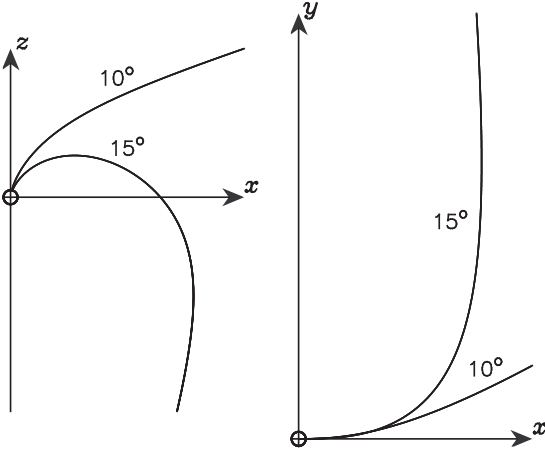


FIG. 6. The particle trajectories on the planes  $(x, z)$  (left panel) and  $(x, y)$  (right panel) for angles  $\vartheta = 10^\circ$  and  $15^\circ$ . The motion is infinite, the direction of the final velocity depends on the initial angle  $\vartheta$ . The circle at the origin of coordinates is the surface of the “star”.

the energy and space distributions of particles taking into account the particle energy losses, changes of their trajectories, etc. This issue we will discuss elsewhere.

Finally, we note that the results of this work are obtained within the framework of classical electrodynamics when the quantum effects can be ignored. If the condition of Eq.(45) is violated, then calculations should be conducted using the methods of quantum theory. If in the initial state the electrons occupies the first level of Landau, then the standard method of calculations used in the quantum theory of synchrotron radiation (see e.g. Ref. [10]) is not applicable since the perpendicular motion cannot be treated as quasi-classical.

#### Appendix A: Trajectories in the field of magnetic dipole

Here we present for illustration the results of numerical calculations of trajectories in the field of the magnetic dipole. The initial Cartesian coordinates of the particle (in units of  $R_*$ ) we set on the sphere of radius  $R_*$  in the form  $\mathbf{r}(0) = (\sin \vartheta, 0, \cos \vartheta)$ ; the initial velocity is directed along the field line, which starts from the point  $\mathbf{r}(0)$ . It is convenient to introduce, instead of  $t$ , a dimensionless parameter  $\tau = t e B_0 / (n c \gamma)$ , where  $B_0$  is the field in the initial point of the trajectory, and write down the equation of motion in the following form

$$\frac{d\boldsymbol{\nu}}{d\tau} = \boldsymbol{\nu} \times \mathbf{b}, \quad \frac{d\mathbf{r}}{d\tau} = \xi \boldsymbol{\nu}. \quad (\text{A1})$$

Here  $\boldsymbol{\nu} = \boldsymbol{\beta}/\beta$  is the unite vector in the direction of velocity,  $\mathbf{b} = \mathbf{B}(\mathbf{r})/B_0$ ,

$$\xi = \frac{m c^2 \gamma \beta}{e B_0 R_*}. \quad (\text{A2})$$

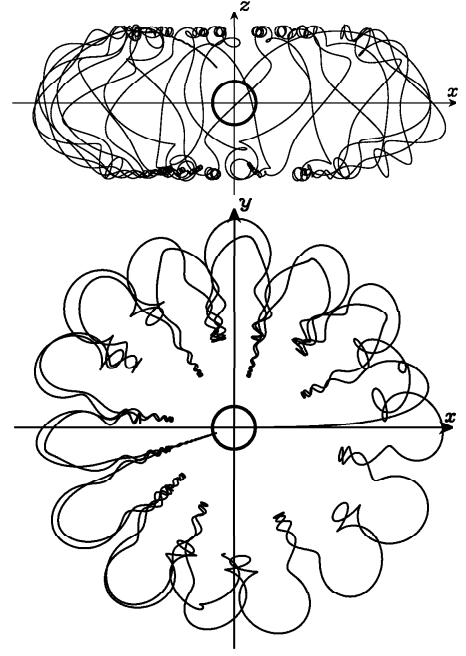


FIG. 7. The same as in Fig. 6, but for angle  $\vartheta = 20^\circ$ .

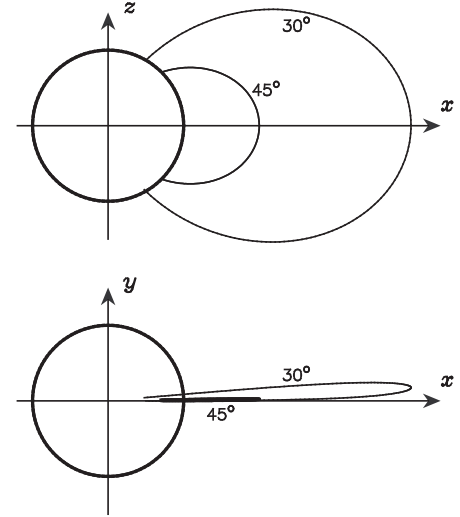


FIG. 8. The same as in Fig. 6, but for angles  $\vartheta = 30^\circ$  and  $45^\circ$ .

Note that only one parameter,  $\xi$ , enters into this equation. In accordance with the condition of Eq.(8), the values of  $1 - \beta$  and  $\xi$  are small compared to unity. We adopted  $\xi = 10^{-3}$ , and performed the calculations without taking into account the effect of radiative friction.

If initially we put the particle on the “pole” and direct the velocity towards the axis  $z$ , the particle apparently will move uniformly along that axis. If at  $t = 0$  the particle is located close to the “pole”, the motion will be not rectilinear, but it will remain infinite (see Fig. 6).

With an increase of  $\vartheta$  the character of motion is dra-

matically changed. For example, at  $\vartheta = 20^\circ$  the particle is trapped by the magnetic field (see Fig. 7). There is no sharp transition between these two cases. At some angles close to  $\vartheta = 20^\circ$ , the particle may make several turns around the star, with a quite chaotic features of motion, and then go to infinity.

At large angles the trajectories are again changed quantitatively, and appear close to the field lines (see Fig. 8). In all cases the initial segment of trajectory ap-

pears close to the field lines; the acceleration on that segment is shown in Fig. 2. Therefore, for the chosen initial conditions the curvature radius of the trajectory significantly differs from the curvature radius of the field line. The initial segments of the trajectory are helical-like lines, but at  $\xi \sim 10^{-3}$  the shift in the perpendicular direction appears of the order of  $10^{-3}$ . Therefore within this uncertainty, the trajectories of particles shown in Figs. 6 – 8 coincide with the smooth trajectories.

- 
- [1] I. P. Ochelkov and V. V. Usov, *Ap&SS* **69**, 439 (1980).
  - [2] L. D. Landau and E. M. Lifshitz, *The Classical Theory of Fields* (Pergamon Press, Oxford, 1975).
  - [3] A. J. Dragt and J. M. Finn, *J. Geophys. Res.* **81**, 2327 (1976).
  - [4] T. Harko and K. S. Cheng, *MNRAS* **335**, 99 (2002), arXiv:astro-ph/0204170.
  - [5] J. D. Jackson, *Classical Electrodynamics* (Wiley, New York, 1998).
  - [6] J. Schwinger, *Phys. Rev.* **75**, 1912 (1949).
  - [7] V. L. Ginzburg and S. I. Syrovatskii, *The origin of cosmic rays* (Gordon and Breach, New York, 1969).
  - [8] F. A. Aharonian, S. R. Kelner, and A. Y. Prosekin, *Phys. Rev. D* **82**, 043002 (2010), arXiv:1006.1045 [astro-ph.HE].
  - [9] R. Buehler, J. D. Scargle, R. D. Blandford, L. Baldini, M. G. Baring, A. Belfiore, E. Charles, J. Chiang, F. D’Ammando, C. D. Dermer, S. Funk, J. E. Grove, A. K. Harding, E. Hays, M. Kerr, F. Massaro, M. N. Mazziotta, R. W. Romani, P. M. Saz Parkinson, A. F. Tennant, and M. C. Weisskopf, *Astrophys. J.* **749**, 26 (2012), arXiv:1112.1979 [astro-ph.HE].
  - [10] E. M. Berestetskii, V. B. Lifshitz and L. P. Pitaevskii, *Quantum Electrodynamics* (Pergamon Press, Oxford, 1989).